

## Supporting Information

### Role of Mo Doping and the Interfacial Interactions Mechanism of Ni-Mo-S Electrodes: the Experimental and Computational Study

Ying Liu<sup>\*, †, a</sup>, Haonan Zhang<sup>†, b</sup>, Xiao Sun<sup>a</sup>, Zheng Xu<sup>a</sup>, Hao Yang<sup>a</sup>, Xiaochun Gao<sup>a</sup>,  
Xitao Yin<sup>a</sup>, Xiaoguang Ma<sup>\*, a</sup>

<sup>a</sup> *Laboratory of Plasma and Energy Conversion, School of Physics and Optoelectronic  
Engineering, Ludong University, Yantai, China*

<sup>b</sup> *College of Physics and Optoelectronic Engineering, Anhui University, Hefei, Anhui  
230601, PR China*

---

\* Corresponding Authors. Tel. number: +86-0535-6672730. E-mail:

liuy2018@ldu.edu.cn (Ying Liu); hsiaoguangma@ldu.edu.cn (Xiaoguang Ma).

† Contributed equally to this work.

Electrochemical performance of NMS-0.5 electrodes is showed in Fig. S1. As shown in Fig. S1a, CV curves of the electrode display typical pseudo-capacitance characteristics with obvious redox peaks. The redox peaks shift slightly as the scanning rate increases from 2 to 100  $\text{mV s}^{-1}$ , which is due to the good conductivity of the electrode. Fig. S1b shows the GCD curves with the current densities range from 5 to 100  $\text{A g}^{-1}$ , the symmetrical charge and discharge curves indicates excellent reversibility of the redox reactions during the energy storage process. The stability of the electrode was detected by GCD and was tested at 40  $\text{A g}^{-1}$  (Fig. S1c). The sample possess long cycling life with 84.5% capacitance retention after 5000 cycles. EIS plots of the NMS-0.5 electrode have negligible change before and after cyclic test, certifying the stable nanostructure of the NMS-0.5 materials.

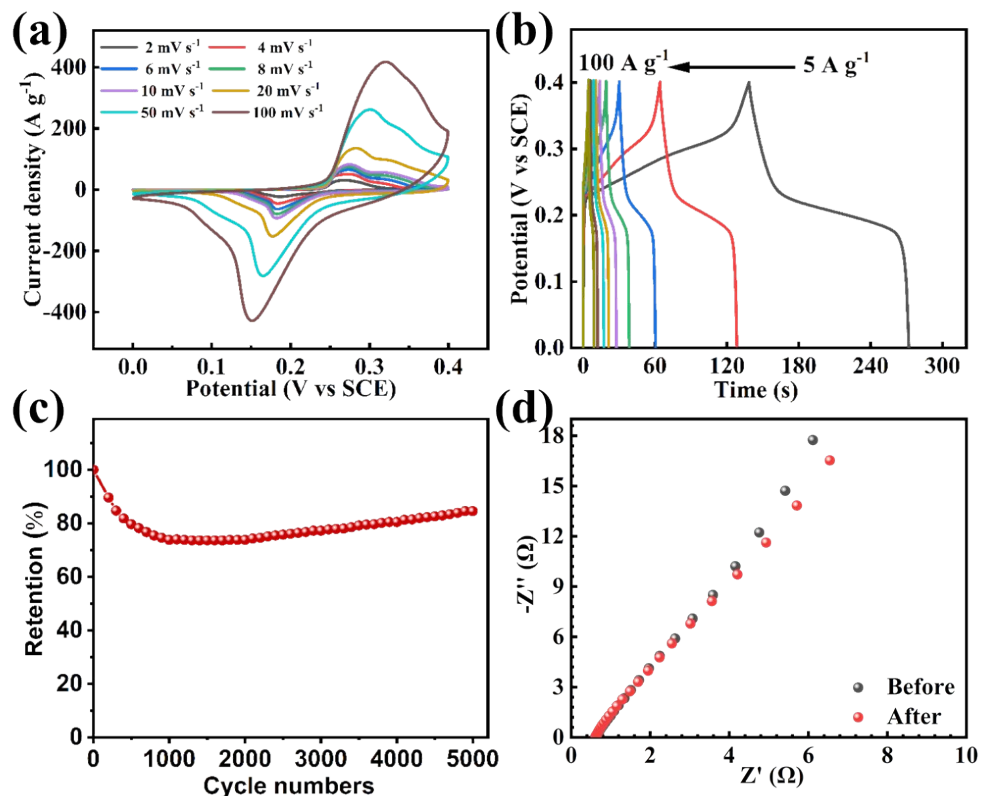


Fig. S1 Electrochemical tests of NMS-0.5 electrodes. (a) CV curves at different scanning speed (2-100 mV s<sup>-1</sup>), (b) GCD curves at current densities from 5 to 100 A g<sup>-1</sup>, (c) stability tested for 5000 cycles, (d) Nyquist plots before and after cyclic test.

The morphological and structural analyses of the NMS-0.5 electrode material were characterized after prolonged cycles. SEM image shows that the nanosheets still uniformly distributed on the Ni foam without agglomeration or rupture after the cycle test (Fig. S2a). Comparing the XRD patterns of the NMS-0.5 materials before and after cyclic test, there're only three typical peaks of Ni foam without other diffraction peaks. Therefore, the crystallinity of NMS materials changes negligible after stability test.

The content and valence state of the elements in NMS-0.5 was studied by XPS analysis. The XPS spectrum verified the NMS sample are composed of Ni, Mo and S elements (Fig. S2c). However, the atomic percent of Ni, Mo, S changed from 12.95%, 3.53%, 7.58% to 19.71%, 0.35%, 3.1% after prolonged cycles. This result may attribute to the redox reaction between  $\text{Ni}^{2+}$  and  $\text{OH}^-$ . The high-resolution Ni 2p spectrum shows two main spin-orbit doublet peaks and two satellite peaks (Fig. S2d). The two peaks located at 855.9 and 873.7 eV indicate the existence of  $\text{Ni}^{2+}$ , the other two deconvoluted peaks at 857.5 and 875.1 eV are assigned to  $\text{Ni}^{3+}$ . Mo 3d spectra features two pairs of peaks at 231.9 and 235.3 eV which are corresponding to  $3d_{5/2}$  and  $3d_{3/2}$  (Fig. S2e). In Fig. S2f, the detailed S 2p spectra displays the binding energy of 162.3 (S  $2p_{3/2}$ ) and 164.1 eV (S  $2p_{1/2}$ ) verifying the Ni-S and Mo-S bonds. In addition, the satellite peak of S around 168.6 eV implies a special high oxidation state of sulfur element. The above characterization studies the morphology, nanostructure, composition, crystalline structure and valence of the NMS nanoflowers after long cycle test, indicating that the structure of the sample is stable, but the content of elements will change due to the redox reactions.

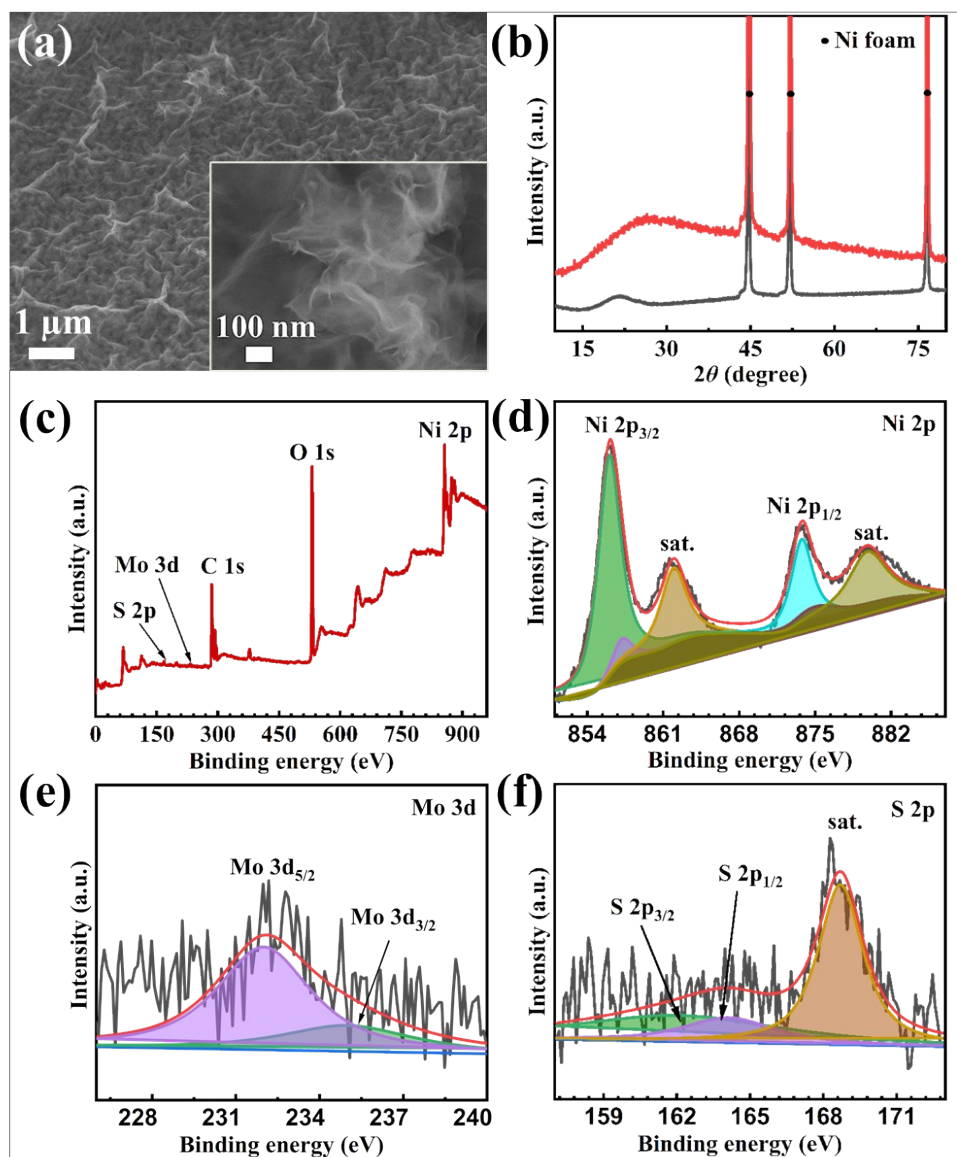


Fig. S2 (a) SEM image of NMS-0.5 materials after 5000 cycles. (b) XRD patterns of NMS-0.5 before (black line) and after (red line) cyclic test. (c) XPS survey spectrum of NMS-0.5 and the high-resolution spectrum of (d) Ni 2p, (e) Mo 3d and (f) S 2p after cyclic test.

To estimate the practical application of the active material NMS-0.5 in supercapacitors, an asymmetric supercapacitor of NMS-0.5//AC was assembled with activated carbon and the NMS-0.5 composite as the negative and positive electrodes (Fig. S3). The electrochemical tests were

operated in a two-electrode system with the potential of 0-1.6 V. The NMS-0.5//AC presents quasi-rectangle shapes with ignorable redox peaks, indicating that the charges of positive and negative electrodes match well (Fig. S3a). The relationship between energy density and power density is reflected in the Ragone plot (Fig. S3b). The assembled asymmetric supercapacitor calculated its energy density and power density by the following formulas:

$$E = 0.5C\Delta V^2/3.6 \quad (1)$$

$$P = 3600E/\Delta t \quad (2)$$

In two-electrode system,  $C$  ( $F\ g^{-1}$ ),  $\Delta V$  ( $V$ ) and  $\Delta t$  ( $s$ ) are on behalf of the specific capacitance, voltage window and the discharge time of the device, respectively. The highest energy density of  $12.0\ Wh\ kg^{-1}$  is exhibited at a power density of  $996.9\ W\ kg^{-1}$ . The power density reaches  $113428.4\ W\ Kg^{-1}$ . Comparing the previously reported composites, RGO/MnO<sub>x</sub> ( $9.4\ Wh\ kg^{-1}$  at  $500\ W\ kg^{-1}$ )<sup>1</sup>, MCs@GNS@NiS ( $11.2\ Wh\ kg^{-1}$  at  $1008\ W\ kg^{-1}$ )<sup>2</sup>, Go-NiCo<sub>2</sub>O<sub>4</sub>//AC ( $7.6\ Wh\ kg^{-1}$  at  $5600\ W\ kg^{-1}$ )<sup>3</sup>. This work present improved electrochemical performance, demonstrating that the NMS-0.5 composites are potential candidate for asymmetric supercapacitor.

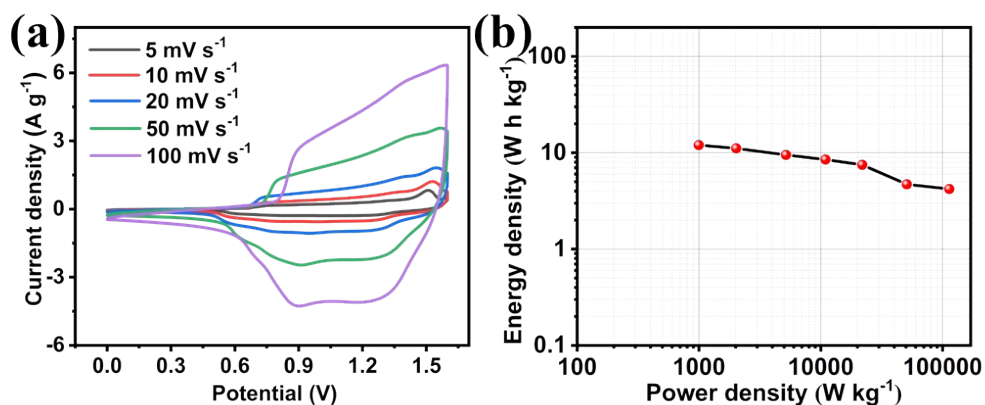


Fig. S3 Electrochemical properties of the NMS-0.5//AC asymmetric device measured in two-electrode system. (a) CV curves at different speeds (5-100 mV s<sup>-1</sup>); (b) the Ragone plot.

### Reference

1. M. Liu, M. Shi, W. Lu, D. Zhu, L. Li and L. Gan, *Chemical Engineering Journal*, 2017, **313**, 518-526.
2. Y. Li, K. Ye, K. Cheng, J. Yin, D. Cao and G. Wang, *Journal of Power Sources*, 2015, **274**, 943-950.
3. H. Wang, C. M. B. Holt, Z. Li, X. Tan, B. S. Amirkhiz, Z. Xu, B. C. Olsen, T. Stephenson and D. Mitlin, *Nano Research*, 2012, **5**, 605-617.